

Promising ZnO-based DSSC performance using HMP  
molecular dyes of high extinction coefficients†Cite this: *Dalton Trans.*, 2014, **43**,  
11305Received 22nd April 2014,  
Accepted 5th June 2014

DOI: 10.1039/c4dt01179a

www.rsc.org/dalton

T. Ganesh,<sup>a</sup> Hong-Minh Nguyen,<sup>a</sup> Rajaram S. Mane,<sup>\*a,b</sup> Nakjoong Kim,<sup>a</sup>  
Dipak V. Shinde,<sup>a</sup> Sambhaji S. Bhande,<sup>b</sup> Mu. Naushad,<sup>c</sup> K. N. Hui<sup>d</sup> and  
Sung Hwan Han<sup>\*a</sup>

Employing newly synthesized di-substituted tri-phenyl amine (HMP-9) and carbazole (HMP-11) dyes (with limited acidic carboxyl anchor groups), a power conversion efficiency as high as 7.03% in ZnO nanocrystallite (NC)-based dye-sensitized solar cells (DSSCs) is achieved. The specific molecular designs of HMP-09 and HMP-11 consisting of with and without hexyloxy spacer groups, and added tri-phenyl amine or 9-phenyl-9H-carbazole donor groups, respectively, attached on the ancillary ligands are advantageous, evidenced from electrochemical impedance spectroscopy measurements, for ZnO NC-based DSSCs.

As promising, low-cost, efficient conversion of visible light into electricity becomes inevitably important, dye-sensitized solar cells (DSSCs), a new class of photoelectrochemical cells based on porous metal oxide semiconductors, Ru-complexes as sensitizers and a liquid electrolyte containing  $\text{I}^-/\text{I}_3^-$ , have attracted significant attention as potential alternatives to conventional Si based solar cells. New molecular sensitizing dyes, in addition to polypyridyl ruthenium compounds of higher extinction coefficients that extend the absorption in the near-infrared region of the solar spectrum are providing better charge generation and transport properties have attracted significant attention.<sup>1,2</sup> Few dyes with amphiphilic heteroleptic characteristics, e.g. Z907, C101 and C106, yielded 9–11% solar-to-electrical conversion efficiencies ( $\eta\%$ ) under 1 Sun illumination.<sup>3</sup> After 20 years of research, the power conversion efficiency of DSSCs has just been increased from 11% to 12.3% in the presence

of a YD2-o-C8 sensitizer and a  $\text{Co}^{\text{II/III}}$  tris(bipyridyl)-based redox electrolyte.<sup>4</sup> It seems that DSSCs based on  $\text{TiO}_2$  reflect the limits imposed by its low electron mobility due to which there is more chance of electron–hole recombination.<sup>5–7</sup> The ZnO nanostructure-based photoanode with similar band gap and conduction band position of the  $\text{TiO}_2$  photoanode suffered from the problems of chemical and thermal stabilities.<sup>8</sup> ZnO forms, *i.e.* morphology, structure and phase, are considered for good electron mobility and electrical conductivity. By Ga doping, 5–6% conversion efficiency of the ZnO photoanode has been reported in the literature,<sup>9</sup> which can be further improved either by surface treatment or by designing the dyes of higher molar extinction coefficients ( $\epsilon$ ).<sup>10</sup> In one of the studies, the ZnO photoanode composed of hierarchically assembled nanocrystallites has been envisaged for record 7.5% power conversion efficiency.<sup>11</sup>

It is quiet accepted that the N719 (*cis*-dithiocyanato-bis(2,2'-bipyridyl-4,4'-dicarboxylate)-ruthenium(II) and N3 sensitizers with 2 and 4 carboxylic acid groups incorporated onto bipyridine ligands, respectively, facilitate anchoring to the photoanode surface and for the transfer of electrons from the dye to the metal oxide (MO) conduction band. In ZnO nanostructure based DSSCs, preventing the formation of the  $\text{Zn}^{2+}$ /dye complex, an insulating layer that eventually blocks the overall electron injection efficiency by producing inferior power conversion efficiency is presently a great challenge.<sup>10</sup> Dye architecture, addition of a donor, conjugated linker groups and electronic coupling between the lowest unoccupied molecular orbital (LUMO) level of the dye and the MO conduction band can enhance the device performance to a greater extent by improving the light harvesting efficiency and charge transport in the photoanode.<sup>12</sup>

With this perspective, herein, we would like to stress the importance of newly designed dye molecules, *cis*-[Ru( $\text{H}_2\text{dcbpy}$ ) (L) (NCS)<sub>2</sub>], where  $\text{H}_2\text{dcbpy}$  = 4,4'-dicarboxylic acid-2,2'-bipyridine and L = 4,4'-bis-(4-di-*p*-hexyloxyphenyl-amino)-styryl-2,2'-bipyridine (HMP-9) and 4,4'-bis-(4-(*N*-carbazolyl)-phenyl-2-vinyl)-2,2'-bipyridine (HMP-11) for efficient ZnO NC-based DSSCs. The obtained conversion efficiencies are superior to Ru( $\text{H}_2\text{dcbpy}$ )

<sup>a</sup>Inorganic Nano-materials Laboratory, Department of Chemistry, Hanyang University, Seongdong-gu, 133791 Seoul, Republic of Korea. E-mail: shhan@hanyang.ac.kr

<sup>b</sup>Centre for Nano-materials & Energy Devices, School of Physical Sciences, SRTM University, 431606 Nanded, India. E-mail: rsmene\_2000@yahoo.com

<sup>c</sup>Advanced Materials Research Chair, Department of Chemistry, College of Science, Building#5, King Saud University, Riyadh, Saudi Arabia

<sup>d</sup>School of Materials Science and Engineering Pusan National University, San 30 Jangjeon-dong, Geumjeong-gu, Busan 609-735, Korea

†Electronic supplementary information (ESI) available: Detailed electrode synthesis, dye synthesis, optical absorption and NMR details. See DOI: 10.1039/c4dt01179a

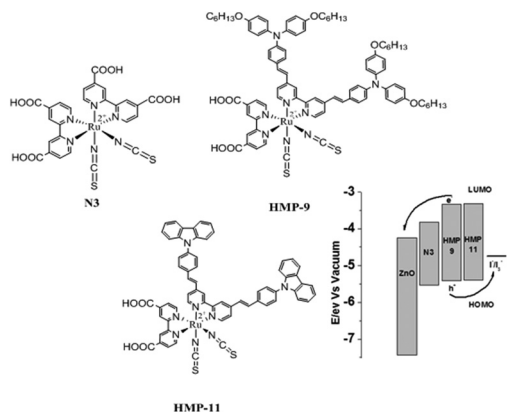


**Fig. 1** Molecular structures and respective energy levels of N3, HMP-9 and HMP-11 sensitizers (for experimental scheme, synthesis procedure and structural characterization, see ESI†).

(4-(4-(*N,N*-di(*p*-hexyloxyphenyl)-amino)styryl)-4'-methyl-2,2'-bipyridine) (NCS)<sub>2</sub>, (HMP-2), recently reported previously<sup>10</sup> and N3 dyes.

Synthetic procedures, structural characteristics, cyclic voltammograms, UV-Vis absorption spectra of HMP-9 and HMP-11 sensitizers can be obtained from the ESI.† Synthesis of ZnO NC photoanodes and DSSC device fabrication details, as well as efficiency measurements are also provided in ESI.† Final molecular structures of these newly *in-lab* designed dyes are shown in Fig. 1. Our previous results on the HMP-2 dye yielded a photo-conversion efficiency of 4.01% where the soaking time for ZnO NC electrodes was as long as 24 h.<sup>13</sup> While designing these new dyes with electron-rich moieties consisting of a planar heterocyclic fused-ring, the carbazole molecule is explored.<sup>14</sup>

The carbazole unit acts as an electron donor to pump the electron to the ruthenium metal in the excited state and improve the power conversion efficiency of DSSCs. Recently, carbazole has been used as an electron donating functional group in organic dyes,<sup>15</sup> where power conversion efficiency is jumped from 6 to 8.3% for TiO<sub>2</sub>-based DSSCs. Here, HMP-9 and HMP-11 dyes with and without hexyloxy spacer groups, and added tri-phenyl amine or 9-phenyl-9*H*-carbazole donor groups, respectively, attached on the ancillary ligands were engineered for optimizing acidity as well as visible light absorption to achieve high efficiency in ZnO-based DSSCs. The extinction coefficients ( $\epsilon$ ) and electrochemical characteristics of HMP dyes are shown in Table 1. There is no noticeable

**Table 1** Photophysical and electrochemical properties of N3 and HMP dyes (vs. vacuum level)

Dye	HOMO (eV)	HOMO-LUMO (eV)	LUMO (eV)	$\lambda_{\max}$ (nm)	$\epsilon$ (M <sup>-1</sup> cm <sup>-1</sup> )
N3	-5.52	1.68	-3.84	530	14 500
HMP 9	-5.41	2.06	-3.35	526	23 576
HMP 11	-5.38	2.05	-3.33	539	21 435

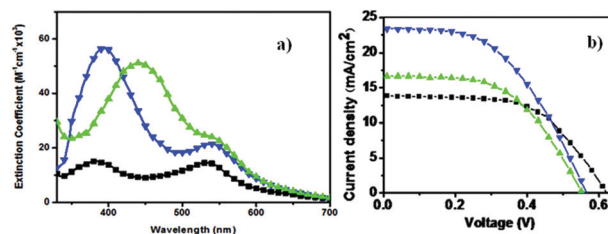


**Fig. 2** (a) Electronic absorption spectra, and (b) *J*-*V* characteristics of the devices employing different dyes. N3 (black, ■), HMP-9 (green, ▲) and HMP-11 (blue, ▼) under the illumination of AM 1.5 G sunlight (100 mW cm<sup>-2</sup>).

difference in the quantity of dyes adsorbed (due to the four hexyloxy chains incorporated on ancillary ligands, the HMP-9 dye has relatively low adsorption compared to the HMP-11 dye) onto ZnO NCs. The replacement of the carboxylic group of the N3 bipyridine ligand site with strong donor functional groups has positively shifted the highest occupied molecular orbital (HOMO) level by 0.22 eV (vs. vacuum level, in HMP-11) which matches well with the redox potential of I<sup>-</sup>/I<sub>3</sub><sup>-</sup>. Whereas, the tri-phenyl amine donor functional group with hexyloxy groups has shifted the HOMO position negatively to 0.11 eV from the N3 dye position. Fig. 2a shows the UV-Vis absorption spectra of the HMP-9 and HMP-11 sensitizers along with the N3 sensitizer (10<sup>-5</sup> M). The absorption spectra of the HMP-9 and HMP-11 sensitizers are dominated by metal-to-ligand charge transfer transitions (MLCT), which are located at two positions, *i.e.* 441 and 526 nm, and 393 and 539 nm, respectively, and the high-energy bands below 320 nm are due to ligand  $\pi$ - $\pi^*$  transitions. The peak position of the MLCT band at 441 nm in the HMP-9 sensitizer is red-shifted compared to HMP-11 and N3. The presence of the carbazole moiety has increased extinction coefficient significantly. The increased  $\pi$ -conjugation length of ancillary ligands with the electron donation functional group in HMP-9 and HMP-11 might be responsible for the increased molar extinction coefficients in the visible region as compared to that of N3. The  $\epsilon$  value of the low-energy MLCT absorption band for HMP-9 and HMP-11 are  $23.5 \times 10^3$  M<sup>-1</sup> cm<sup>-1</sup> and  $21.4 \times 10^3$  M<sup>-1</sup> cm<sup>-1</sup>, respectively, which are significantly higher than the corresponding values for the N3 ( $14.5 \times 10^3$  M<sup>-1</sup> cm<sup>-1</sup>). Whereas other bands observed at 441 and 393 nm wavelength regions show significant improvement in absorption characteristics peculiar to the nature of the dye donor molecular characteristics. A blue shift of 9 nm along with 3.76 times higher  $\epsilon$  values of the HMP-11 sensitizer compared to N3 would certainly fascinate its uniqueness in the DSSC's performance. Fig. 2b presents the typical current-voltage (*J*-*V*) spectra of the designed HMPs and N3 dyes immobilized on the ZnO NC photoanodes.

Devices sensitized with HMP-11 exhibited a highest short circuit current density ( $J_{sc}$ ) of 23.4 mA cm<sup>-2</sup> and an overall power conversion efficiency ( $\eta$ %) of 7.09%, whereas those sensitized with HMP-9 and N3 exhibited efficiencies of 5.34 and 4.94% (Table 2). All measurements were performed without mask. Open circuit voltage ( $V_{oc}$ ) is almost same in all the cases.

**Table 2** The standard device electronic parameters extracted from the  $J$ - $V$  data for N3 and HMP dyes (onto ZnO NCs-based photoanodes)

Dye	$J_{sc}$ (mA cm <sup>-2</sup> )	$V_{oc}$ (V)	ff	$\eta\%$
N3	13.8	0.61	0.58	4.94
HMP-9	16.7	0.58	0.55	5.34
HMP-11	23.4	0.61	0.49	7.09

The high photocurrent in HMP-11 sensitized devices is attributed to its high extinction coefficient which increases its light harvesting efficiency and to the superior electron transport through the device. We believe that further improvement in  $V_{oc}$  and fill factor (ff) values can be achieved using surface treatment such as 4-*tert*-butylpyridine, Li(CF<sub>3</sub>SO<sub>2</sub>)<sub>2</sub>N and forming the core-shell structures, *etc.*<sup>16,17</sup>

As seen in Fig. 3a, the photocurrent action spectra show the highest spectral response for the red shifted HMP-11 dye with a peak incident photon-to-current conversion efficiency (IPCE) of about 77% at 464 nm. The HMP-9 dye with four hydrophobic hexyloxy substituents attached to impede the tri-iodide ions from reaching the ZnO NC surface and to prevent molecular aggregation due to  $\pi$ - $\pi$  stacking, disadvantageously, has reduced the IPCE value to 51%. This is due to an intermolecular quenching or clouding of long alkyl, non-conjugated, hexyloxy substituents that generally diminish the light absorption by the filtering effect. Despite the higher  $\epsilon$  in HMP-9, it exhibits lower IPCE and  $\eta\%$  (discussed later) values suggesting that there is a need of indepth investigation on the charge generation, collection and recombination kinetics across electrolyte/dye/ZnO NC/indium-tin-oxide (ITO) interfaces. The maximum IPCE value of the HMP-11 dye is supposed to be obtained from better MLCT and hole conducting carbazole moieties. Electrochemical impedance spectroscopic (EIS) analysis is often performed to understand the interfacial charge transfer resistance, electron transport rate and recombination effect in DSSCs.<sup>18</sup> Impedance spectra of DSSCs generally exhibit three semicircles. A small semicircle at a high frequency region corresponds to the interface between platinum and the electrolyte, a big semicircle in the intermediate frequency range corresponds to photoanode-electrolyte interface whereas one in the low frequency range is related to Warburg impedance of the electrolyte. Fig. 3b shows the Nyquist plots of ZnO NC-

based DSSCs with dyes, considered in the present study, under 1 Sun illumination and open circuit voltage conditions. It is clear from the figure that photoanodes utilizing N3 and HMP-11 dyes demonstrate higher recombination resistance values confirming high electron lifetimes and obviously more photoconversion efficiencies. On the other hand, the photoanode utilizing the HMP-9 dye has lower recombination resistance and thus electron recombination will be higher and lifetime will be lower.<sup>19,20</sup> The HMP-11 dye with an electron rich carbazole moiety aids in superior electron transport within the device, and thus is expected to produce higher power conversion efficiency.

In summary, dye-sensitized solar cells utilizing ZnO NCs with newly synthesized di-substituted tri-phenyl amine (HMP-9) and carbazole (HMP-11) as donor moieties on bipyridine ligands with limited acidic carboxyl anchoring groups in addition to the routinely used N3 dye are investigated, where electron-rich donor moieties increased the extinction coefficient and improved charge generation and transportation abilities. The ZnO NC electrode sensitized with the HMP-11 dye demonstrated as high as 7.05% power conversion efficiency with a better short current density of  $\sim 23.4$  mA cm<sup>-2</sup>, under simulated AM 1.5, 100 mW cm<sup>-2</sup> illumination. Electrochemical impedance measurements revealed that the devices constructed utilizing newly synthesized dyes, with and without hexyloxy spacer groups, and added tri-phenyl amine or 9-phenyl-9*H*-carbazole donor groups attached on the ancillary ligands have improved charge generation and transport properties than N3 dye. It would be interesting to use gel electrolyte<sup>21</sup> and compact metal oxide layers of relatively high band gaps<sup>22</sup> for improving both the stability and performance.

The authors wish to thank the Basic Science Research Program through the National Research Foundation of Korea (NRF), funded by the Ministry of Education (2013009768). Authors (R.S. Mane and Mu. Naushad) also extend their gratitude to the Visiting Professor (VP) unit of King Saud University (KSU) for their kind support.

## References

- 1 F. Gao, Y. Wang, D. Shi, J. Zhang, M. Wang, X. Jing, R. Humphry Baker, P. Wang, S. M. Zakeeriddin and M. Gratzel, *J. Am. Chem. Soc.*, 2008, **130**, 10720.
- 2 J. J. Cid, J. H. Yum, S. R. Jang, M. K. Nazeeriddin, E. Martinez-ferrero, E. Palomares, J. Ko, M. Gratzel and T. Torres, *Angew. Chem., Int. Ed.*, 2007, **46**, 8358.
- 3 Y. Cao, Y. Bai, Q. Yu, Y. Cheng, S. Liu, D. Shi, F. Gao and P. Wang, *J. Phys. Chem. C*, 2009, **113**, 6290.
- 4 A. Yella, H. W. Lee, H. N. Tsao, C. Yi, A. K. Chandiran, M. K. Nazeeruddin, E. W. G. Diau, C. Y. Yeh, S. M. Zakeeruddin and M. Gratzel, *Science*, 2011, **334**, 629.
- 5 F. Xu and L. Sun, *Energy Environ. Sci.*, 2011, **4**, 418.
- 6 Z. Ning, Y. Fu and H. Tian, *Energy Environ. Sci.*, 2010, **3**, 1170.
- 7 H. Snaith, *Energy Environ. Sci.*, 2012, **5**, 653.

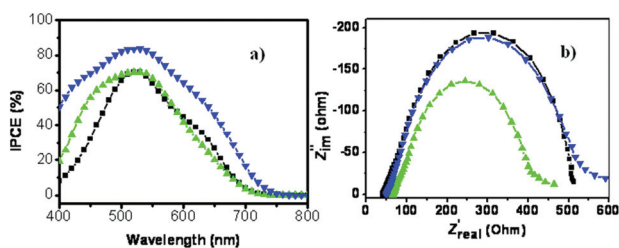


**Fig. 3** (a) Photocurrent action spectra and (b) EIS Nyquist plots measured under open circuit conditions in 1 Sun illumination for the devices employing different dyes. N3 (black, ■), HMP-9 (green, ▲) and HMP-11 (blue, ▼).

- 8 Q. Zhang, T. P. Chou, B. Russo, S. A. Jenekhe and G. Cao, *Adv. Funct. Mater.*, 2008, **18**, 1654.
- 9 Q. Zhang, T. P. Chou, B. Russo, S. A. Jenekhe and G. Cao, *Angew. Chem., Int. Ed.*, 2008, **47**, 2402.
- 10 H. M. Nguyen, R. S. Mane, T. Ganesh, S. H. Han and N. Kim, *J. Phys. Chem. C*, 2009, **113**, 9206.
- 11 N. Memarian, I. Concina, A. Braga, S. M. Rozati, A. Vomiero and G. Sberveglieri, *Angew. Chem., Int. Ed.*, 2011, **50**, 12321.
- 12 P. Docampo, S. Guldin, T. Leijtens, N. K. Noel, U. Steiner and H. J. Snaith, *Adv. Mater.*, 2014, DOI: 10.1002/adma.201400486.
- 13 T. Ganesh, R. S. Mane, G. Cai, J. Chang and S. H. Han, *J. Phys. Chem. C*, 2009, **113**, 7666.
- 14 J. V. Grazulevicius, P. Strohhriegl, J. Pielichowski and K. Pielichowski, *Prog. Polym. Sci.*, 2003, **28**, 1297.
- 15 N. O. V. Plank, S. J. Snaith, C. Ducati, J. S. Bendall, L. Schmidt-Mende and M. E. Welland, *Nanotechnology*, 2008, **19**, 465603.
- 16 C. Y. Chen, J. G. Chen, S. J. Wu, J. Y. Li, C. G. Wu and K. C. Ho, *Angew. Chem., Int. Ed.*, 2008, **120**, 7452.
- 17 N. Koumura, Z. S. Wang, M. Mori, M. Miyashita, E. Suzuki and J. Hara, *J. Am. Chem. Soc.*, 2006, **128**, 14256.
- 18 C. He, L. Zhao, Z. Zheng and F. Lu, *J. Phys. Chem. C*, 2008, **112**, 18730.
- 19 R. Zhu, C. Y. Jiang, B. Liu and S. Ramkrishna, *Adv. Mater.*, 2009, **21**, 994.
- 20 W. Lee, S. K. Min, V. Dhas, S. B. Ogale and S. H. Han, *Electrochem. Commun.*, 2009, **11**, 103.
- 21 G. L. D. Gregorio, R. Agosta, R. Giannuzzi, F. Martina, L. D. Marco, M. Manca and G. Gigli, *Chem. Commun.*, 2012, **48**, 3109.
- 22 N. O. V. Plank, I. Howard, A. Rao, M. W. B. Wilson, C. Ducati, R. S. Mane, J. S. Bendall, R. R. M. Louca, N. C. Greenham, H. Miura, R. Friend, H. J. Snaith and M. E. Welland, *J. Phys. Chem. C*, 2009, **29**, 18515.